Available online at www.sciencedirect.com
SCIENCE DIRECT®
Journal of Sound and Vibration 277 (2004) 931–941
JOURNAL OF SOUND AND VIBRATION
www.elsevier.com/locate/jsvi

Unbiased expression of FRF with exponential window function in impact hammer testing

Se Jin Ahn, Weui Bong Jeong*, Wan Suk Yoo

Vibration and Noise Laboratory, School of Mechanical Engineering, Pusan National University, 30 Changjeon-Dong, Kumjeong-Ku, Pusan 609-735, South Korea

Received 7 February 2003; accepted 22 September 2003

Abstract

The exponential window function is widely used in impact hammer testing to reduce leakage errors as well as to get a nice S/N ratio. The larger the exponential decay rate of the window is, the more effectively the leakage errors are reduced. But if the decay rate of the exponential window function is too large, the frequency response function (FRF) is distorted by its side effects. The modal parameters of the system cannot be exactly identified from the distorted FRF even though modal analysis technique is used. Therefore, it is a difficult problem to determine a proper exponential decay rate in an impact hammer testing.

In this paper, the amount of the FRF distortion caused by the exponential window function is theoretically uncovered, and an unbiased expression of the exponential-windowed FRF is represented. A new circle fitting method is also proposed so that the modal parameters are directly extracted from the impulse response spectrum distorted by the exponential window function. The results identified by the conventional and proposed circle fitting method are compared through numerical examples.

1. Introduction

The impulse input like the impact hammer is widely used in vibration test fields to obtain the frequency response function (FRF) because of its convenience and simplicity for experiments [1–5]. In most of the conventional analyzers, however, the signals acquired from impact hammer testing have been dealt with as periodic and stationary although they are obviously neither periodic nor stationary. Therefore, the FRFs obtained by the impact hammer testing contain some serious errors, such as finite record-length errors and leakage errors, when the signal data

*Corresponding author. Tel.: +82-51-510-2337; fax: +82-51-517-3805.
E-mail address: wbjeong@pusan.ac.kr (W.B. Jeong).

0022-460X/$ - see front matter
doi:10.1016/j.jsv.2003.09.022

for digital signal processing (DSP) is not sufficiently long [6–8]. There have been attempts to reduce these errors by using various window functions [9–11]. The exponential window function is generally used to reduce leakage errors and to get a nice S/N ratio of the signals in impact hammer testing [12]. However, the decay rate of the exponential window function applied to the impulse response signal causes distortion of the widowed FRF. The damping ratio of the system cannot be completely recovered from the exponential-windowed FRF although modal analysis techniques are properly used.

This paper theoretically shows that the exponential window function used in impact hammer testing makes the FRF distorted even though it helps reduce leakage errors as well as finite record-length errors. The exact formulation of the exponential-windowed FRF has to be expressed to calculate the unbiased modal parameters of a dynamic system. The unbiased expression of FRF with exponential window function is theoretically derived in this paper. A new circle fitting method using the unbiased formulation is also developed so that the modal parameters can be directly calculated from the exponential-windowed FRF. Finally, numerical examples of a 1-d.o.f. model verify the validity and usefulness of the developed circle fitting method.

2. Finite record-length errors in unit impulse response function

The equation of motion of a viscously damped 1-d.o.f. system of Fig. 1 is described as follows:

$$m\ddot{x}(t) + c\dot{x}(t) + kx(t) = f(t). \tag{1}$$

If the force in the right hand side of Eq. (1) is impulse, it can be expressed by the Dirac delta function

$$f(t) = F_0\delta(t). \tag{2}$$

The response of displacement under impulse input of Eq. (2) can be described as [13,14]

$$x(t) = F_0 h(t) = F_0 \frac{e^{-\zeta\omega_n t}}{m\omega_d} \sin \omega_d t, \quad t \geqslant 0, \tag{3}$$

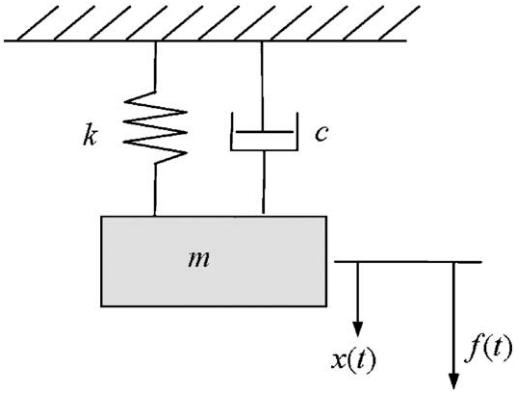

Fig. 1. Damped 1-d.o.f. vibration model.

where $h(t)$ means unit impulse response function. Since the signal cannot be obtained for an infinite time period, it should be modified for a record length, T_{RL}. In this case, the Fourier transformation of the impulse signal can be written as [15]

$$F(\omega)|_{T_{RL}} = \int_{-\infty}^{\infty} f(t)\mathrm{e}^{-\mathrm{j}\omega t}\,\mathrm{d}t = F_0 \int_0^{T_{RL}} \delta(t)\mathrm{e}^{-\mathrm{j}\omega t}\,\mathrm{d}t = F_0. \tag{4}$$

Since the spectrum of impulsive force has constant values over the entire frequency range, it has no relation to the record length. On the other hand, the Fourier transformation of $x(t)$ in Eq. (3) becomes

$$\begin{aligned} X(\omega)|_{T_{RL}} &= \int_{-\infty}^{\infty} x(t)\mathrm{e}^{-\mathrm{j}\omega t}\,\mathrm{d}t = F_0 \int_0^{T_{RL}} \frac{\mathrm{e}^{-\zeta\omega_n t}}{m\omega_d}\sin\omega_d t\mathrm{e}^{-\mathrm{j}\omega t}\,\mathrm{d}t \\ &= \frac{F_0}{k-\omega^2 m+\mathrm{j}\omega c}[1-E(\omega)|_{T_{RL}}], \end{aligned} \tag{5}$$

where

$$E(\omega)|_{T_{RL}} = \mathrm{e}^{-\zeta\omega_n T_{RL}}\,\mathrm{e}^{\mathrm{j}\omega T_{RL}}\left\{\frac{\zeta}{\sqrt{1-\zeta^2}}\sin\omega_d T_{RL}+\cos\omega_d T_{RL}+\mathrm{j}\frac{\omega}{\omega_d}\sin\omega_d T_{RL}\right\} \tag{6}$$

represents a finite record-length error in this paper. If record length T_{RL} were sufficiently large, the FRF would be calculated as

$$H(\omega) = \lim_{T_{RL}\to\infty}\frac{X(\omega)|_{T_{RL}}}{F(\omega)|_{T_{RL}}} = \frac{1}{k-\omega^2 m+\mathrm{j}\omega c} = \frac{1/k}{1-(\omega/\omega_n)^2+\mathrm{j}2\zeta(\omega/\omega_n)}. \tag{7}$$

This means that the FRF obtained from impact hammer testing would match its exact FRF in the case of an infinitely long record length. However, a finite record-length error is not actually avoidable because record length is inevitably finite.

3. FRF distortion caused by exponential window function

The exponential window function is usually applied to impulse response signal in order to reduce finite record-length errors and leakage errors which take place when the record length is not sufficiently long. The characteristics of a windowed FRF will be discussed in this section. If an exponential window function with decay rate σ is applied to Eq. (3), we can write

$$h_w(t) = \mathrm{e}^{-\sigma t}\frac{\mathrm{e}^{-\zeta\omega_n t}}{m\omega_d}\sin\omega_d t, \quad t\geqslant 0. \tag{8}$$

When the time data is acquired for record length T_{RL}, the Fourier transformation of Eq. (8) is described as

$$\begin{aligned} \tilde{H}_w(\omega)\big|_{T_{RL}} &= \int_0^{T_{RL}} \mathrm{e}^{-\sigma t}\frac{\mathrm{e}^{-\zeta\omega_n t}}{m\omega_d}\sin\omega_d t\,\mathrm{e}^{-\mathrm{j}\omega t}\,\mathrm{d}t \\ &= \frac{1/k}{1-(\omega/\omega_n)^2+2\zeta(\sigma/\omega_n)+(\sigma/\omega_n)^2+\mathrm{j}2(\zeta+\sigma/\omega_n)(\omega/\omega_n)}[1-E_w(\omega)|_{T_{RL}}], \end{aligned} \tag{9}$$

where

$$E_w(\omega)|_{T_{RL}} = e^{-(\sigma/\omega_n+\zeta)\omega_n T_{RL}}[(\omega/\omega_n)\sin\omega_d T_{RL}\sin\omega\, T_{RL} + (\sigma/\omega_n+\zeta)(\omega_n/\omega_d)\cos\omega_d T_{RL}\sin\omega T_{RL} + \cos\omega_d T_{RL}\cos\omega T_{RL} + j\{(\omega/\omega_n)\sin\omega_d T_{RL}\cos\omega T_{RL} - (\sigma/\omega_n+\zeta)(\omega_n/\omega_d)\sin\omega_d T_{RL}\sin\omega T_{RL} - \cos\omega_d T_{RL}\sin\omega T_{RL}\}]. \quad (10)$$

The $E_w(\omega)|_{T_{RL}}$ given in Eq. (10) represents the finite record-length error. The relation between the absolute values of $E_w(\omega_n)|_{T_{RL}}$ and the ratio of the exponential decay rate to natural angular velocity σ/ω_n, is shown in Fig. 2. Specifically, Fig. 2(a) shows their relations according to the changes in the number of the signal's periods existing in record length $f_n \times T_{RL}$, when the damping ratio ζ is fixed as 0.01. Fig. 2(b) shows the relation according to the changes of the damping ratio when the number of the signal's periods $f_n \times T_{RL}$ is fixed as 20. From Fig. 2, we can see that the finite record-length error is inevitably involved in the frequency response spectrum when the damping ratio of the signal is relatively small or when the record length is not sufficiently long. The larger the decay rate of the applied window becomes, the smaller the error becomes. Hence, the error $E_w(\omega)$ will become infinitesimal in case that record length is sufficiently long or the decay rate of the exponential window function is sufficiently large. When the finite record-length error $E_w(\omega)$ is removed by selecting a large decay rate of the exponential window function, the windowed FRF becomes

$$\bar{H}_w(\omega)\big|_{T_{RL}} = \frac{1/k}{1-(\omega/\omega_n)^2 + 2\zeta(\sigma/\omega_n) + (\sigma/\omega_n)^2 + j2(\zeta+\sigma/\omega_n)(\omega/\omega_n)}. \quad (11)$$

Until now it has been known that the decay rate σ of the exponential window function affects only the damping ratio ζ of the FRF in Eq. (7), and the effect of the decay rate can be removed by the conventional modal analysis technique [3,13,14]. But Eq. (11) proposed in this paper shows that the exponential-windowed FRF is different from the exact FRF given in Eq. (7), although the

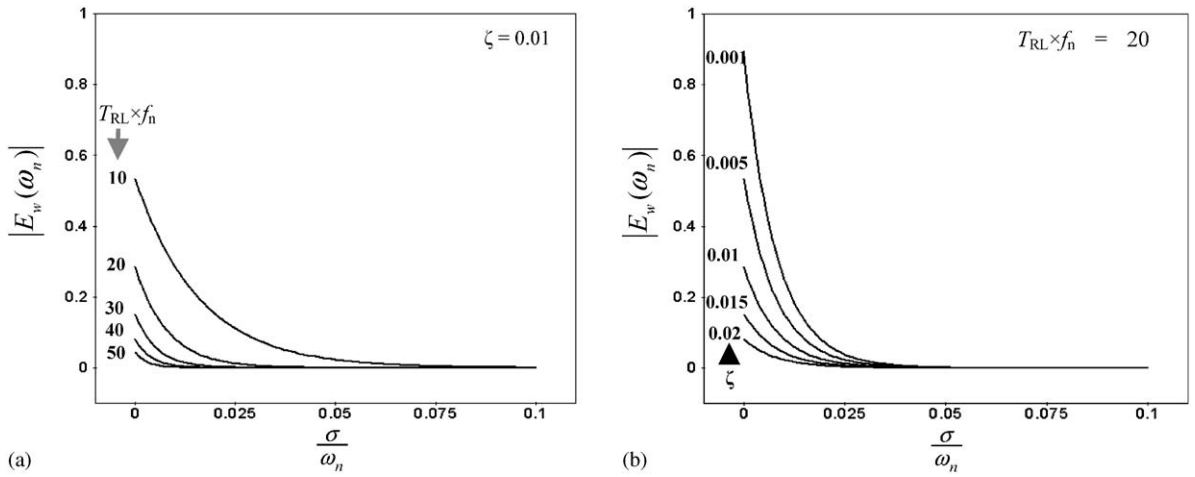

Fig. 2. Errors of Eq. (10) according to changes of exponential decay ratio of window function. (a) Fixing damping ratio and (b) fixing the number of signals within record length.

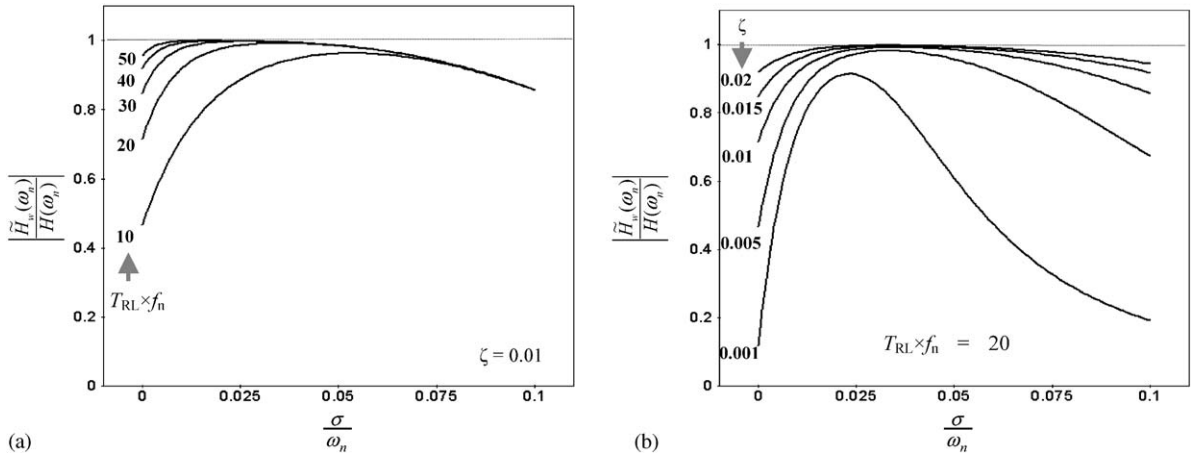

Fig. 3. Ratio of peak amplitudes of windowed FRF to exact FRF at natural frequency according to changes of decay rate of exponential window function. (a) Fixing damping ratio and (b) fixing the number of signals within record length.

effect of decay rate in the imaginary part of the denominator of Eq. (11) is exactly removed by the modal analysis technique.

The exponential-windowed FRF given in Eq. (9) shows that although the finite record-length error $E_w(\omega)$ is diminished by the large decay rate, the FRF becomes distorted because of the third and forth term of its denominator. On the contrary, in the case of a small decay rate, a finite record-length error which is not completely removed makes the FRF incorrect. Therefore, it is not true that modal parameters can be exactly derived from the exponential-windowed FRF.

The absolute value of the ratio of the exact FRF given in Eq. (7) to the windowed FRF given in Eq. (9) is shown in Fig. 3. Specifically, Fig. 3(a) shows the values according to changes of the number of the signal's periods existing in record length $f_n \times T_{RL}$, when the damping ratio ζ is fixed as 0.01. Fig. 3(b) show the values according to changes of the damping ratio when the number of the signal's periods $f_n \times T_{RL}$ is fixed as 20. As shown in Fig. 3, the finite record-length error is further and further diminished until the decay rate of the exponential window function reaches a specific value. But when the decay rate is larger than a specific value, the FRF is gradually more distorted because of the window effect. There are some cases where the exact FRF cannot be obtained in spite of using any suitable exponential window function. Therefore, it is necessary to develop a new method by which the exact FRF can be directly estimated from the exponential-windowed FRF with any decay rate.

4. A new circle fitting method for exponential-windowed FRF

The mobility of the FRF given in Eq. (11) is expressed as

$$\bar{Y}(\omega) = \mathrm{j}\omega \times \bar{H}_w(\omega)\big|_{T_{RL}} = \mathrm{Re}[\bar{Y}(\omega)] + \mathrm{j}\,\mathrm{Im}[\bar{Y}(\omega)], \tag{12}$$

where the real and imaginary parts are given by

$$\mathrm{Re}[\bar{Y}(\omega)] = \frac{\omega/k\{2(\zeta+\sigma/\omega_n)(\omega/\omega_n)\}}{\{1-(\omega/\omega_n)^2+2\zeta(\sigma/\omega_n)+(\sigma/\omega_n)^2\}^2+\{2(\zeta+\sigma/\omega_n)(\omega/\omega_n)\}^2}, \tag{12a}$$

$$\mathrm{Im}[\bar{Y}(\omega)] = \frac{\omega/k\{1-(\omega/\omega_n)^2+2\zeta(\sigma/\omega_n)+(\sigma/\omega_n)^2\}}{\{1-(\omega/\omega_n)^2+2\zeta(\sigma/\omega_n)+(\sigma/\omega_n)^2\}^2+\{2(\zeta+\sigma/\omega_n)(\omega/\omega_n)\}^2}, \tag{12b}$$

respectively. The real and imaginary parts in the conventional circle fitting method have simpler expressions written as

$$\mathrm{Re}[\bar{Y}(\omega)] = \frac{\omega/k\{2(\zeta+\sigma/\omega_n)(\omega/\omega_n)\}}{\{1-(\omega/\omega_n)^2+\{2(\zeta+\sigma/\omega_n)(\omega/\omega_n)\}^2},$$

$$\mathrm{Im}[\bar{Y}(\omega)] = \frac{\omega/k\{1-(\omega/\omega_n)^2\}}{\{1-(\omega/\omega_n)^2+\{2(\zeta+\sigma/\omega_n)(\omega/\omega_n)\}^2}.$$

Rearranging Eq. (12) gives the equation of the modal circle as

$$\{\mathrm{Re}[\bar{Y}(\omega)]-c\}^2+\mathrm{Im}[\bar{Y}(\omega)]^2=c^2, \tag{13}$$

where

$$c=\frac{\omega_n/k}{4(\zeta+\sigma/\omega_n)}. \tag{14}$$

The equation of the modal circle can be determined by using the least square estimation to minimize the sum of errors given by

$$\text{Sum of errors}=\sum_{\omega}\{\mathrm{Re}[\bar{Y}(\omega)]-\mathrm{Re}[S(\omega)]\}^2+\sum_{\omega}\{\mathrm{Im}[\bar{Y}(\omega)]-\mathrm{Im}[S(\omega)]\}^2, \tag{15}$$

where $S(\omega)$is the mobility obtained by experiments such as the impact hammer testing. It is calculated as follows:

$$S(\omega)=\mathrm{j}\omega\times\frac{DFT[x(t)\times \mathrm{e}^{-\sigma t}]}{DFT[f(t)]}. \tag{16}$$

The Nyquist plot of a system and its modal circle calculated from Eq. (15) are shown in Fig. 4. The frequency ω_0, where the magnitude of mobility has the maximum value, can be obtained by the simplest interpolation equation as

$$\omega_0=\omega_a+\frac{\theta_a}{\theta_a+\theta_b}(\omega_b-\omega_a). \tag{17}$$

In Eq. (17), ω_a and ω_b represent the frequencies near the peak on the Nyquist plot. A higher order interpolation technique can be used to get more precise results.

Using both Eq. (12) and Fig. 4, the following equations can be derived:

$$\tan\theta_a=\frac{1+2\zeta(\sigma/\omega_n)+(\sigma/\omega_n)^2-(\omega_a/\omega_n)^2}{2(\zeta+\sigma/\omega_n)(\omega_a/\omega_n)}\geqslant 0, \tag{18}$$

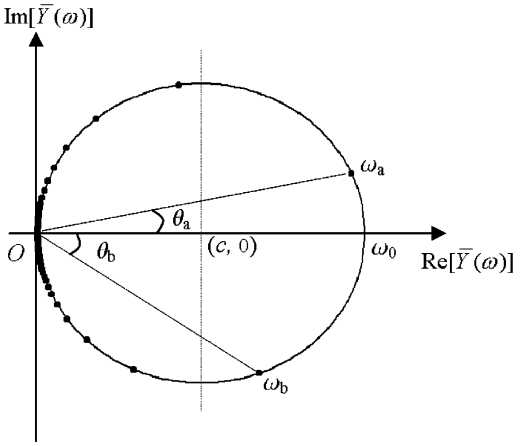

Fig. 4. Point data from Nyquist plot and the modal circle of mobility with exponential window function.

$$\tan\theta_b = \frac{(\omega_b/\omega_n)^2 - \{1 + 2\zeta(\sigma/\omega_n) + (\sigma/\omega_n)^2\}}{2(\zeta + \sigma/\omega_n)(\omega_b/\omega_n)} \geqslant 0. \tag{19}$$

To derive the damping ratio ζ, the sum of the above equations is presented as

$$\tan\theta_a + \tan\theta_b = \frac{\{1 + 2\zeta(\sigma/\omega_n) + (\sigma/\omega_n)^2\} + (\omega_a/\omega_n)(\omega_b/\omega_n)(\omega_b/\omega_n - \omega_a/\omega_n)}{2(\zeta + \sigma/\omega_n)(\omega_a/\omega_n)(\omega_b/\omega_n)}. \tag{20}$$

If Eq. (20) is rearranged, the damping ratio can be directly calculated by

$$\zeta = \frac{[\omega_b/\omega_n - \omega_a/\omega_n][1 + (\sigma/\omega_n)^2 + ((\omega_b/\omega_n)(\omega_a/\omega_n))] - 2(\tan\theta_a + \tan\theta_b)(\sigma/\omega_n)(\omega_a/\omega_n)(\omega_b/\omega_n)}{2(\tan\theta_a + \tan\theta_b)(\omega_a/\omega_n)(\omega_b/\omega_n) - 2[\omega_b/\omega_n - \omega_a/\omega_n](\sigma/\omega_n)}. \tag{21}$$

Using $\mathrm{Im}[\bar{Y}(\omega = \omega_0)] = 0$ as shown in Fig. 4, the following quadratic equation is given:

$$\omega_n^2 + 2\sigma\zeta\omega_n - \omega_0^2 + \sigma^2 = 0. \tag{22}$$

Substituting ς of Eq. (21) into Eq. (22), the natural angular frequency $\omega_n$is calculated from

$$\omega_n^2 = \omega_0^2 + \sigma^2 - \frac{\sigma(\omega_0^2 + \omega_a\omega_b)(\omega_b - \omega_a)}{(\tan\theta_a + \tan\theta_b)\omega_a\omega_b}. \tag{23}$$

The natural angular frequency in the conventional circle fitting method has the following form:

$$\omega_n^2 = \omega_0^2,$$

which is much simpler than Eq. (23). The modal stiffness k can be calculated by the following equation rearranged from Eq. (14):

$$k = \frac{\omega_n}{4\zeta c}. \tag{24}$$

After the modal parameters are calculated by the new circle fitting method developed in this paper, an improved FRF is obtained by applying them to Eq. (7).

5. Numerical example

In order to discover the relation between finite record-length errors and decay rate of the exponential window function, a 1-d.o.f. damped model shown in Fig. 1 is simulated as shown. Using the Runge–Kutta method, the response of the displacement to impulsive excitation $f(t)$ is calculated for the system which has mass m of 3.0 kg, spring constant k of 47,374.1 N/m, damping coefficient c of 11.3 N s/m, natural frequency f_n of 20 Hz, and damping ratio ζ of 0.015. The impulse force and its displacement response are plotted in Fig. 5. The modal parameters are

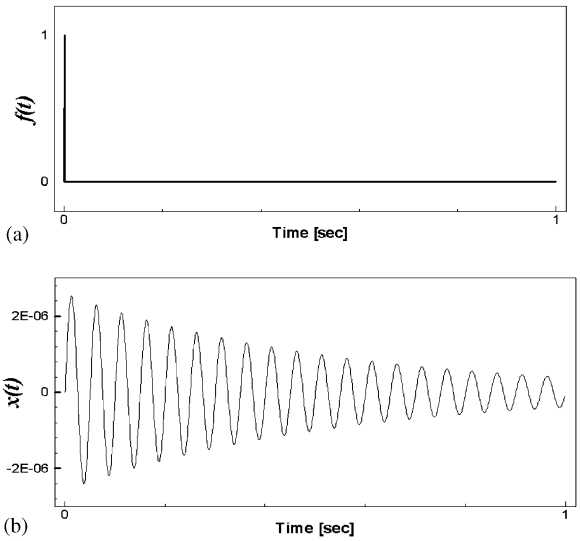

Fig. 5. Impulse and response signals of 1-d.o.f. vibration model. (a) Impulse force and (b) displacement response.

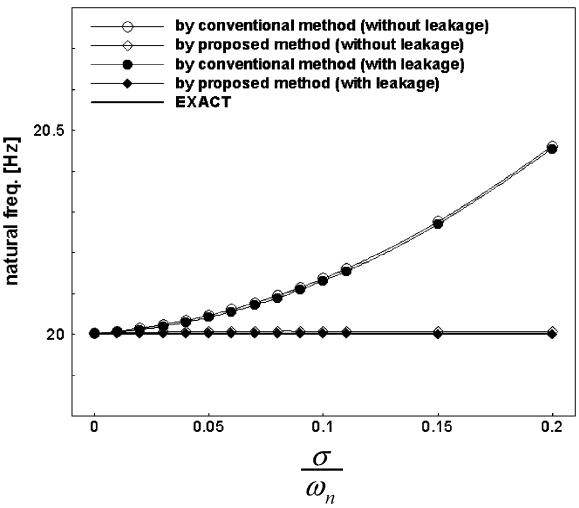

Fig. 6. Comparison of natural frequency estimated by the conventional and proposed circle fitting methods.

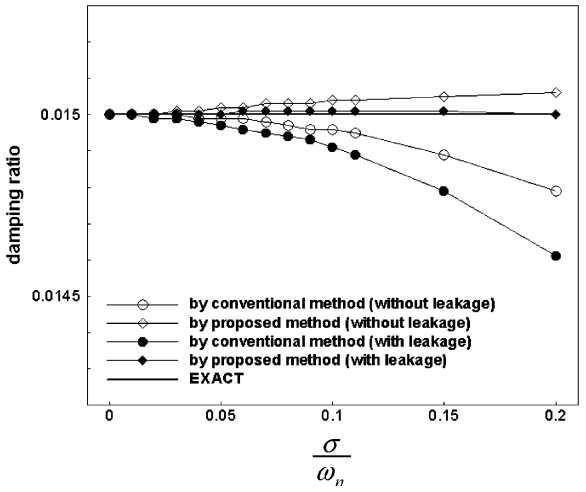

Fig. 7. Comparison of damping ratio estimated by the conventional and proposed circle fitting methods.

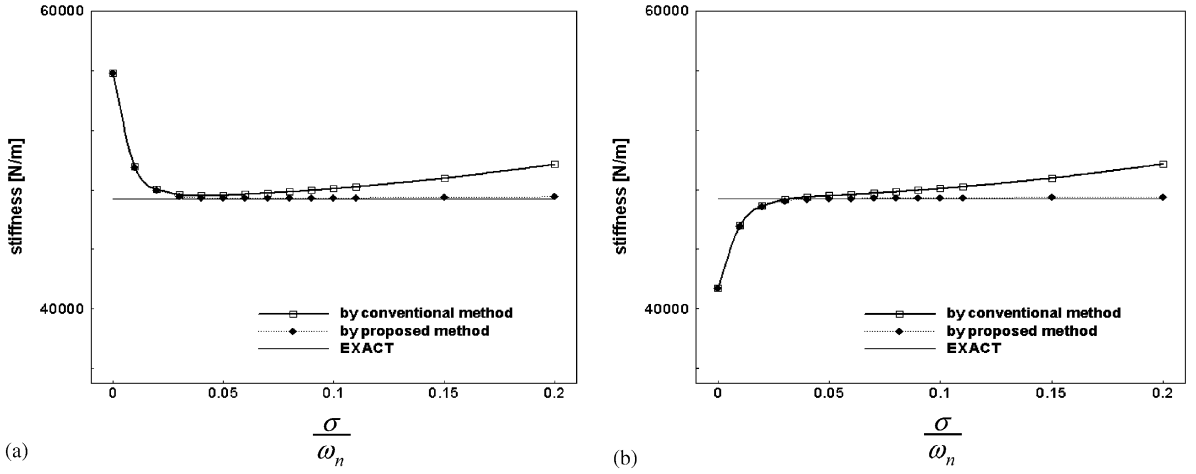

Fig. 8. Comparison of stiffness of the model estimated by the conventional and proposed circle fitting methods. (a) Without leakage and (b) with leakage.

calculated by the conventional circle fitting method and by the new method proposed in this paper, and compared in Figs. 6–8. The term 'without leakage' in these figures represents that the record length exactly matches to the period time of the signal. The term 'with leakage' represents that the record length does not match the period. These figures show that the proposed circle fitting method estimates the natural frequency and damping ratio of the numerical model well regardless of the decay rate of the exponential window function applied to the signal. The FRFs obtained by the conventional and by the proposed circle fitting methods in the case of $\sigma/\omega_n = 0.2$ are compared in Fig. 9. While the FRF obtained by the conventional method differs from the exact FRF, the FRF by the proposed method agrees with the exact FRF.

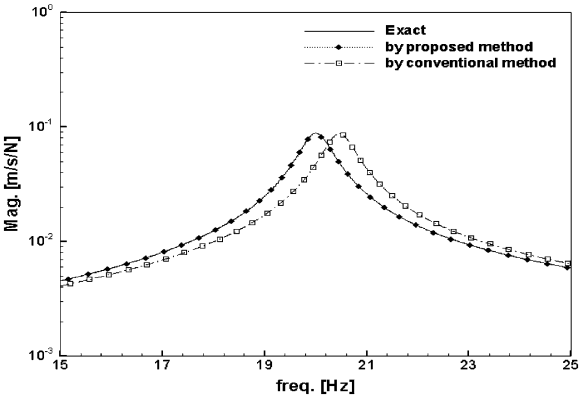

Fig. 9. Comparison of FRF by the conventional and proposed methods. ($\sigma/\omega_n = 0.2$).

6. Conclusions

1. The finite record-length error in the impulse response spectrum is formulated theoretically.
2. Although the exponential window function reduces finite record-length errors as well as leakage errors, it causes other kinds of errors which distort the windowed FRF.
3. If the decay rate of the exponential window function is relatively small, the finite record-length errors are not effectively reduced. In the case of a large decay rate, the windowed FRF is distorted again by the side effects of the exponential window function.
4. A new circle fitting method is developed to estimate the correct modal parameters directly from the exponential-windowed FRF.
5. The proposed method is validated through numerical examples, and the effectiveness of the method is verified.

Acknowledgements

The authors would like to thank the Ministry of Science and Technology of Korea for the financial support by a grant (M1-0203-00-0017) under the NRL (National Research Laboratory).

References

[1] P.K. Roy, N. Ganesan, Transient response of a cantilever beam subjected to an impulse load, *Journal of Sound and Vibration* 183 (5) (1995) 873–890.
[2] A.J. Stanley, N. Ganesan, Impulse response of cylindrical shells with a discontinuity in the thickness subjected to an axisymmetric load, *Journal of Sound and Vibration* 184 (3) (1995) 369–387.
[3] D.J. Ewins, *Modal Testing: Theory and Practice*, Research Studies Press, Baldock, Hertfordshire, UK, 1986.
[4] R.B. Randall, Frequency analysis, B & K Ltd., Denmark, 1987.
[5] K.G. McConnell, *Vibration Testing: Theory and Practice*, Wiley, New York, 1995.

[6] W.B. Jeong, S.J. Ahn, H.Y. Chang, C.H. Chang, The improvement of leakage error in digital Fourier transform, *Journal of the Korean Society for Noise and Vibration Engineering* 11 (3) (2001) 455–460.
[7] S.J. Ahn, W.B. Jeong, The errors and reducing method in 1-dof frequency response function from impact hammer testing, *Journal of the Korean Society for Noise and Vibration Engineering* 12 (9) (2002) 702–708.
[8] S.J. Ahn, W.B. Jeong, The improvement of muti-dof impulse response spectrum by using optimization technique, *Journal of the Korean Society for Noise and Vibration Engineering* 12 (10) (2002) 792–798.
[9] J.C. Burgess, On digital spectrum analysis of periodic signals, *Journal of the Acoustical Society of America* 58 (3) (1975) 556–567.
[10] Z.L. Qiu, A.K. Tieu, A method to obtain exact frequency characteristics of harmonic signals, *Mechanical Systems and Signal Processing* 13 (3) (1999) 523–529.
[11] H. Dishan, Phase error in fast Fourier transform analysis, *Mechanical System and Signal Processing* 9 (2) (1995) 113–118.
[12] W. Fladung, R. Rost, Application and correction of the exponential window for frequency response function, *Mechanical Systems and Signal Processing* 11 (1) (1997) 23–36.
[13] A. Nagamatsu, *Modal Analysis*, Baifukan, Japan, 1985.
[14] N.M.M. Maia, J.M.M. Silva, *Theoretical and Experimental Modal Analysis*, Research Studies Press, Baldock, Hertfordshire, UK, 1998.
[15] J.S. Bendat, A.G. Piersol, *Random Data: Analysis and Measurement Procedures*, Wiley, New York, 1986.